Arabian Journal of Chemistry (2021) **14**, 103154

King Saud University

Arabian Journal of Chemistry

www.ksu.edu.sa
www.sciencedirect.com

ORIGINAL ARTICLE

Design, multistep synthesis and *in-vitro* antimicrobial and antioxidant screening of coumarin clubbed chalcone hybrids through molecular hybridization approach

Sathish Kumar Konidala [a,b], Vijay Kotra [c], Ravi Chandra Sekhara Reddy Danduga [a], Phani Kumar Kola [a,*], Richie R. Bhandare [d,e,*], Afzal B. Shaik [f,*]

[a] *University College of Pharmaceutical Sciences, Acharya Nagarjuna University, Nagarjuna Nagar, Guntur, A.P. 522510, India*
[b] *Department of Pharmaceutical Sciences, Vignan's Foundation for Science, Technology, and Research, Guntur, Andhra Pradesh, India*
[c] *Faculty of Pharmacy, Quest International University Perak (QIUP), Malaysia*
[d] *Department of Pharmaceutical Sciences, College of Pharmacy & Health Sciences, Ajman University, PO Box 346, Ajman, United Arab Emirates*
[e] *Center of Medical and Bio-allied Health Research, Ajman University, Ajman, United Arab Emirates*
[f] *Department of Pharmaceutical Chemistry, Vignan Pharmacy College, Jawaharlal Nehru Technological University, Vadlamudi 522213, Andhra Pradesh, India*

Received 10 March 2021; accepted 4 April 2021
Available online 15 April 2021

KEYWORDS

Coumarin;
Chalcone;
Coumarin clubbed chalcone;
Hybrids;
Antimicrobial;
Antioxidant

Abstract In the present study we designed and synthesized 26 coumarin clubbed chalcone hybrids (**1**–**13** and **14**–**26**) in good yields (54.32–74.25%) and further tested for their antimicrobial and antioxidant activities considering the potential bioactivities of these two pharmacophores. All Spectroscopic techniques including FT-IR, ^{1}H NMR, ^{13}C NMR and mass were used to characterize the compounds. The antimicrobial and antioxidant activities of these compounds were performed by agar well diffusion method and DPPH free radical assay respectively. The compounds elicited considerable antimicrobial and potential antioxidant activities. Bioactivity data designated that the

* Corresponding authors at: University College of Pharmaceutical Sciences, Acharya Nagarjuna University, Nagarjuna Nagar, Guntur, A.P. 522510, India (P.K. Kola); Department of Pharmaceutical Sciences, Vignan's Foundation for Science, Technology, and Research, Guntur, Andhra Pradesh, India and Department of Pharmaceutical Sciences, College of Pharmacy & Health Sciences, Ajman University, PO Box 346, Ajman, United Arab Emirates (R.R. Bhandare); Department of Pharmaceutical Chemistry, Vignan Pharmacy College, Jawaharlal Nehru Technological University, Vadlamudi 522213, Andhra Pradesh, India (A.B. Shaik).
E-mail addresses: drphanikumarkola@gmail.com (P.K. Kola), r.bhandareh@ajman.ac.ae (R.R. Bhandare), bashafoye@gmail.com (A.B. Shaik).
Peer review under responsibility of King Saud University.

Production and hosting by Elsevier

https://doi.org/10.1016/j.arabjc.2021.103154

compounds **1** and **7** with no and 4-Cl substitution on the phenyl ring of coumarin clubbed chalcones with 3,4-dihydropyrimidine-2-one displayed antibacterial activity with minimum inhibitory concentration (MIC) value of 10 μM and 17 μM against *Staphylococcus aureus* and MIC value of 8 μM and 13 μM against *Escherichia coli* and antifungal activity with MIC value of 10 μM and 11 μM against *Aspergillus niger* respectively. On the other hand, coumarin clubbed chalcones with 3,4-dihydropyrimidine-2(1H)-thione scaffold (**14**–**26**) exhibited potential antioxidant activity. Among them, compounds **22** containing electron releasing 2-OH substituent was the most active with 77.92% scavenging activity, followed by **14** and **26** (75.22% and 71.32%). The promising leads evolved through this investigation are important for the future development of novel and potential antioxidant compounds.

1. Introduction

Molecular hybridization (MH) is one of the commonly employed drug design strategy by medicinal chemists for the design and development of new lead compounds. This approach will yield novel molecules that can interact with multiple sites through unique molecular interactions. MH tactic will potentiate the biological activity of the newly generated pharmacophores and reduce the side effects associated with the individual components (Bruch et.al., 2011). In addition, MH can lead to generation of compounds with altered pharmacokinetic profiles, selectivity, dual and/or different mechanism of actions as well as the greater biological activity (Viegas-Junior et al., 2007). Furthermore, the molecular hybrids produced are rigid scaffolds that have effective interactions with the target.

Coumarins are a type of natural products and are chemically 2H-chromen-2-one derivatives that belongs to a class of natural products known as benzopyrones (Venugopala et.al., 2013, Menezes et.al., 2019, Barot et al., 2015). This scaffold is present in drugs including vitamin K antagonistic anticoagulants-warfarin, dicumarol, acenocoumarol and DNA gyrase inhibitor antibiotic-novobiocin (cathomycin/albamycin) (Ufer, 2005, Cesar et.al., 2004, Holbrook et.al., 2005, Gellert et.al., 1976, Sugino et.al., 1978). Chalcones are another type of natural products containing C_6-C_3-C_6 arrangement and are a kind of open chain flavonoids. Chalcone scaffold has attracted the scientists across the globe and many reviews have highlighted the biological and synthetic utility of these compounds (Yazdan et.al., 2015, Gaonkar et.al., 2017, Zhuang et al., 2017, Habib, 2018). Chalcone scaffold is found in clinically approved drugs including metochalcone

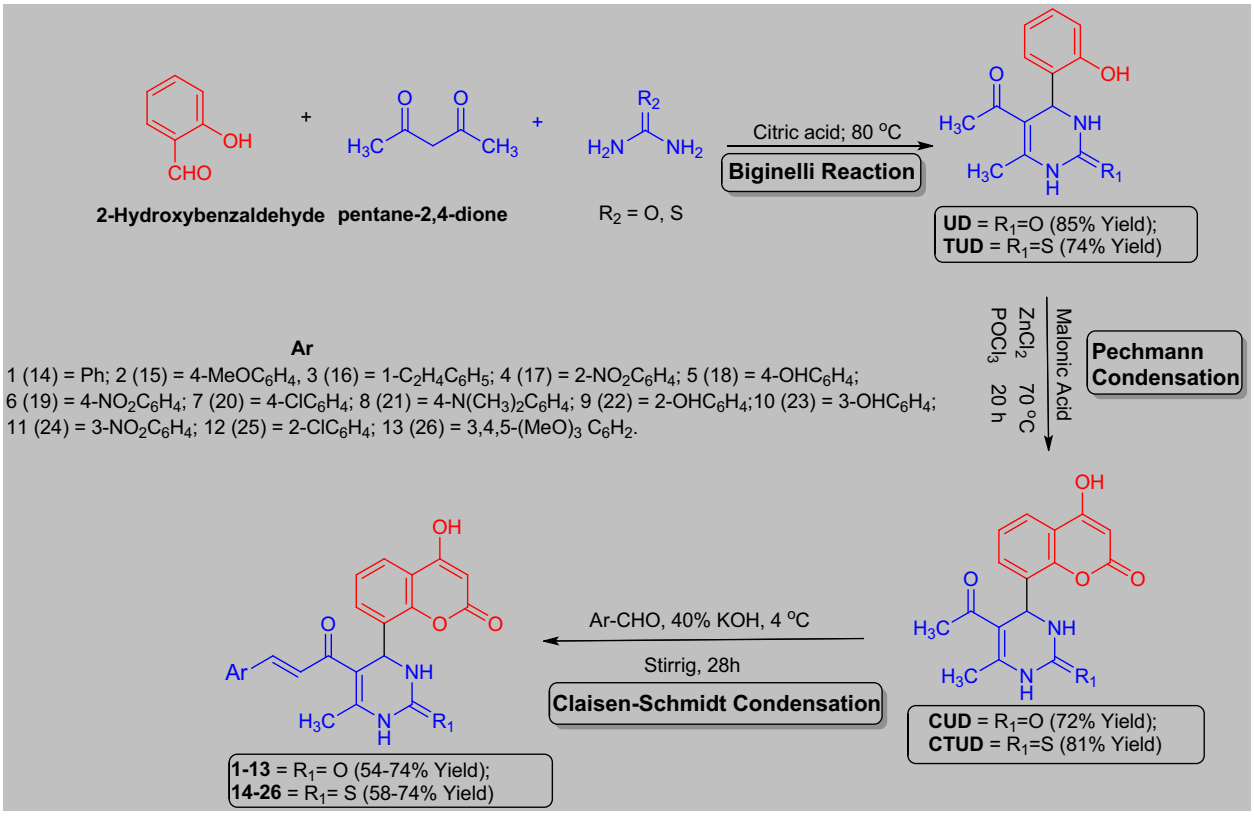

Scheme 1 Synthetic protocol for the preparation of target coumarin clubbed chalcone hybrids (**1**–**13** and **14**–**26**).

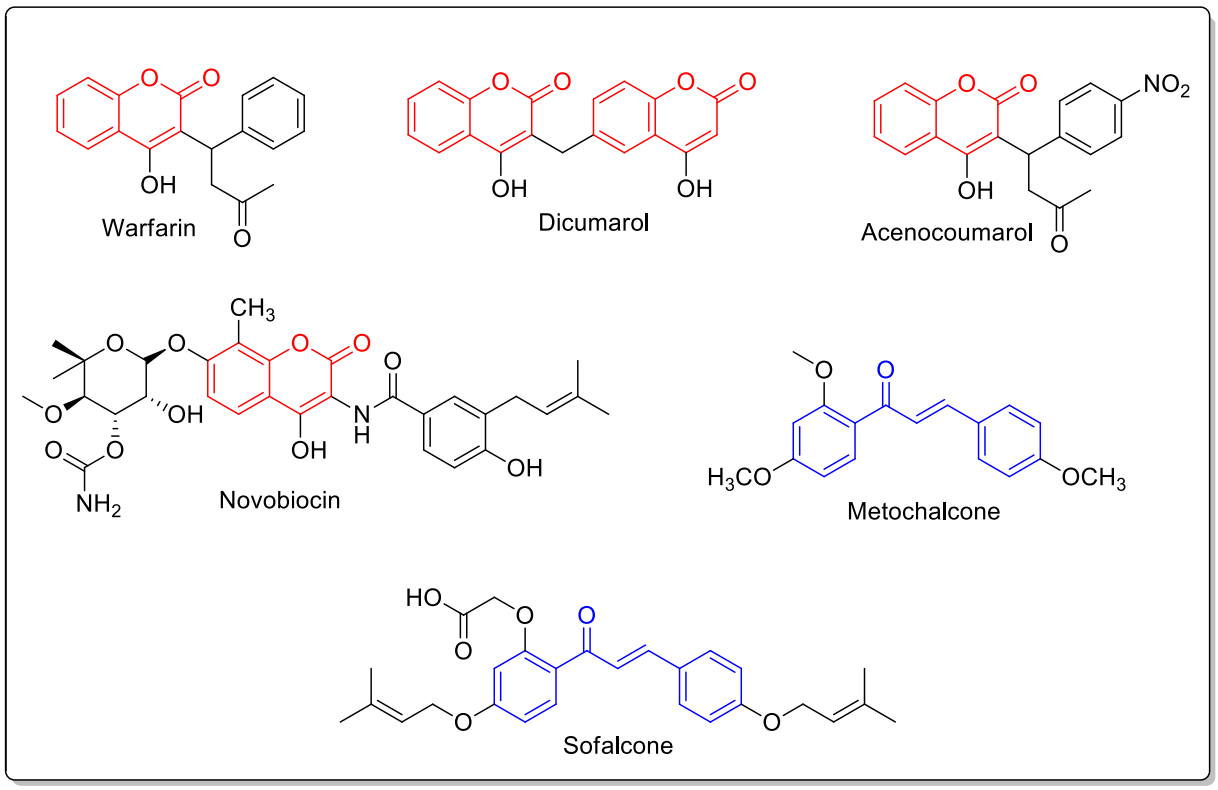

Fig. 1 Structures of clinically useful coumarin and chalcone derivatives.

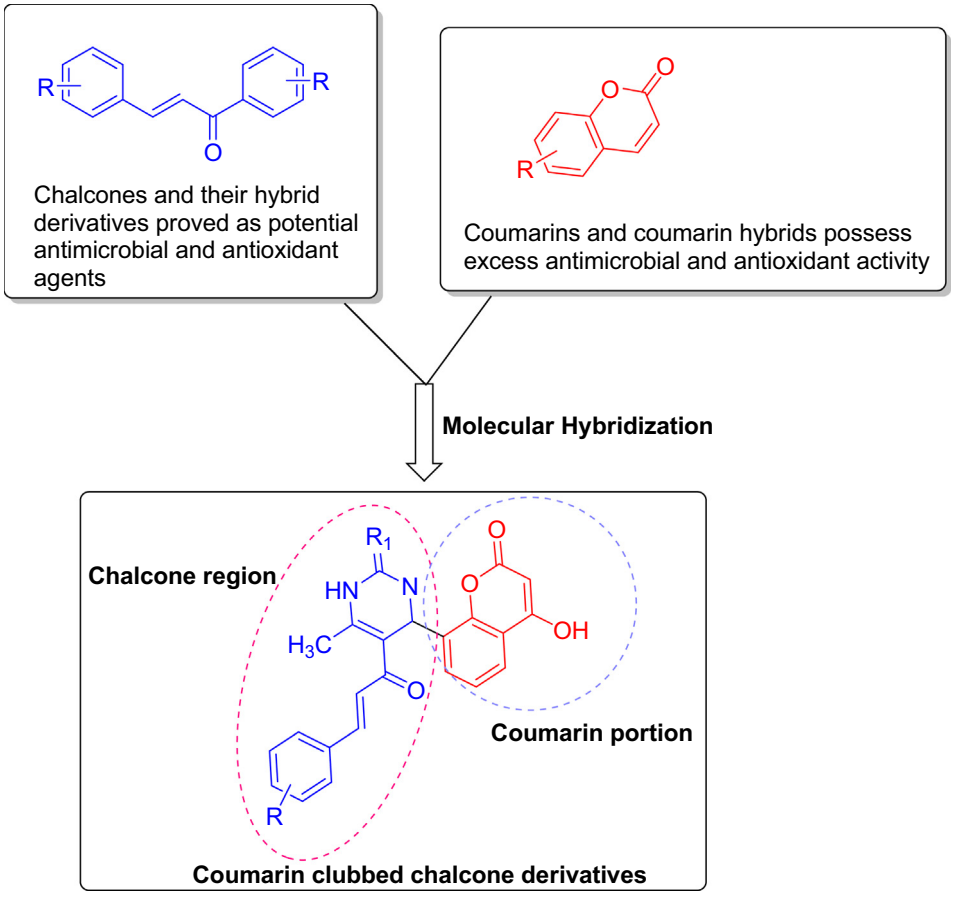

Fig. 2 Design strategy for coumarin clubbed chalcone hybrids.

Table 1 Physical and spectral properties of coumarin-chalcone hybrids ***(1–13)***.

Compound Code	Chemical Structure/Formula	Appearance	% Yield	Melting Point (°C)	Spectral data
UD	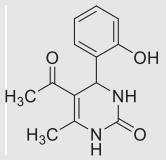	Colorless crystals	85	112–114	MS [*m*/*z*, %]: 247 (M + 1, 14.8). FT-IR (cm^{-1}, KBr): v 1671.24 (C═O), 1734.41 (C═O), 2925.58 (C─H), 3060.07 (Ar─C─H), 3370.82 (N─H), 3479.58 (O─H). ^{1}H NMR (400 MHz, DMSO d_6, ppm): 2. 28 (s, 3H, C─H), 2. 35 (s, 3H, C─H─C═O), 4. 91 (s, 1H, C─H), 6. 83–7. 86 (m, 5H, aromatic), 9.03 (s, 1H, O─H), 9.71 (s, 1H, O─H). ^{13}C NMR (100 MHz, DMSO d_6, ppm): 41. 8 (C─H), 27. 3 (Me), 19. 4 (Me), 106. 2–128. 7 (Ar─C), 145. 4 (CN), 154. 2 (C─O),150. 7 (C═O), 192. 5 (C═O).
CUD	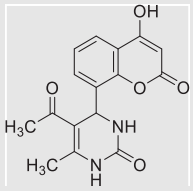	Brick red crystals	72	102–104	MS [*m*/*z*, %]: 315 (M + 1, 18.1) FT-IR (cm^{-1}, KBr): v 1665.38 (C═O), 1732.21 (C═O), 2928.32 (C─H), 3038.55 (Ar─C─H), 3362 (N─H), 3456.29 (O─H). ^{1}H NMR (400 MHz, DMSO d_6, ppm): 2. 23 (s, 3H, C─H), 2. 32 (s, 3H, C─H), 5. 09 (s, 1H, C─H), 6. 82–7. 69 (m, 5H, aromatic), 9. 06 (s, 1H, N─H), 9. 88 (s, 1H, O─H). ^{13}C NMR (100 MHz, DMSO d_6, ppm): 42. 3 (C─H), 19. 27. 40 (Me), 71 (Me), 91. 6–128. 2, (Ar─C), 145. 1 (CN), 150. 2, 162. 1, 192. 3 (C═O), 166.8 (C─O)
1	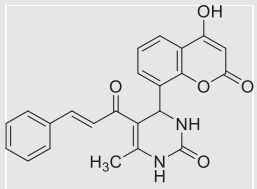 $C_{23}H_{18}N_2O_5$	Yellow solid	66	91–93	MS [*m*/*z*, %]: 403 (M + 1, 25.6). FT-IR (cm^{-1}, KBr): v 1057.01, 1282.03, (C─O─C), 1474.89, 1601.26 (C═C), 1671.61 (C═O), 1734.27 (C═O), 2925.46 (C─H), 3060.24 (Ar─C─H), 3370.44 (O─H), 3479.20 (N─H). ^{1}H NMR (400 MHz, DMSO d_6, ppm): 2. 50 (s, 3H, C─H), 4. 95 (s, 1H, C─H), 6. 91 (s, 2H, N─H) 7. 42–7.65 (m, 9H, Ar), 8. 32 (d, 2H, H─C═C─H), 9. 11 (s, 1H, O─H). ^{13}C NMR (100 MHz, DMSO d_6, ppm): 42. 5 (C─C─H), 17. 7 (CH_3), 117. 4, – 154. 8 (Ar─C), 142. 2 (C═C), 150. 2, 162. 2, 193. 3 (C═O), 166. 1(CO).
2	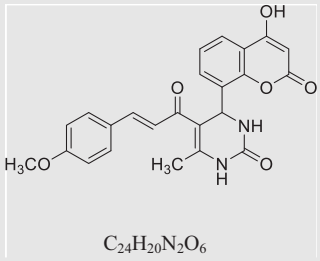 $C_{24}H_{20}N_2O_6$	Dark red solid	57	107–109	MS [*m*/*z*, %]: 433 (M + 1, 26.4). FT-IR (cm^{-1}, KBr): v 830.66 (o-sub), 1024.16, 1252.28 (C─O─C), 1474.34, 1611.30 (C═C), 1665.06 (C═O), 1732.89 (C═O), 2840.59 (C─H), 2928.48 (Ar─C─H), 3362.42 (O─H), 3436.40 (N─H). ^{1}H NMR (400 MHz, DMSO d_6, ppm): 2. 54 (s, 3H, C─H), 3. 78 (s, 3H, C─ H), 4. 91 (s, 1H, C─H), 6.9 (s, 2H, N─H), 7. 34–7. 84 (m, 8H, Ar), 8. 37 (d, 2H, H─C═C─H), 9.11 (s, 1H, O─H). ^{13}C NMR (100 MHz, DMSO d_6, ppm): 54. 3 (C─H), 42. 2 (C─C─H), 17. 9 (CH_3), 91. 4, – 159. 2 (Ar─C), 142. 6 (C═C), 150. 4, 162. 6, 193. 5 (C═O), 166. 5 (C─O).
3	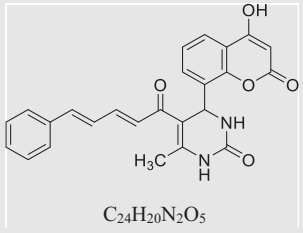 $C_{24}H_{20}N_2O_5$	Yellow Solid	54	98–100	MS [*m*/*z*, %]: 429 (M + 1, 27.5). FT-IR (cm^{-1}, KBr): v 1057.08, 1256.20 (C─O─C), 1602.23, 1474.92 (C═C), 1674.44 (C═O), 2923.58 (C─H), 3038.25 (Ar─C─H), 3269.81 (O─H), 3462.92 (N─H). ^{1}H NMR (400 MHz, DMSO d_6, ppm): 2. 48 (s, 3H, C─H), 4. 74 (s, 1H, C─H), 6. 12 (s, 2H, N─H), 6. 62–7. 41 (m, 9H, Ar), 7. 82 (d, 4H, C═C), 9. 05 (s, 1H, O─H). ^{13}C NMR (100 MHz, DMSO d_6, ppm): 42. 1 (C─C─H), 17. 6 (Me), 91. 2–154. 2 (Ar─C), 141. 3, 151. 4 (C═C), 150. 1, 162. 4 193. 2 (C═O), 166. 6 (C─O).
4		Green solid	70	135–137	MS [*m*/*z*, %]: 448 (M + 1, 25.3). FT-IR (cm^{-1}, KBr): v 756.09 (o-sub), 1236.52 (C─O─C), 1384.47, 1531.29 (NO_2), 1608.38 (C═C), 1672.94 (C═O), 2925.35 (C─H), 3042.09 (Ar─C─H), 3378.02 (O─H),

Table 1 (*continued*)

Compound Code	Chemical Structure/Formula	Appearance	% Yield	Melting Point (°C)	Spectral data
	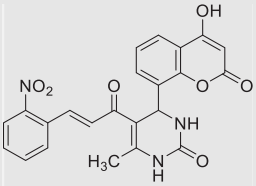 $C_{23}H_{17}N_3O_7$				3445.29 (N—H). ^{1}H NMR (400 MHz, DMSO d_6, ppm): 2. 49 (s, 3H, C—H), 4. 93 (s, 1H, C—H), 7. 10 (s, 2H, N—H) 7. 36–8. 10 (m, 8H, Ar), 8. 45 (d, 2H, H—C═C—H), 9. 09 (s, 1H, O—H). ^{13}C NMR (100 MHz, DMSO d_6, ppm): 42.7 (C—C—H), 18.3 (Me), 91.2–154.1 (Ar—C), 147.3 (C—N), 152.6 (C═C), 166.3 (C—O), 150.5, 162.8, 193.5 (C═O).
5	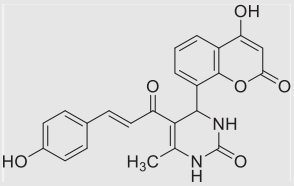	Brown solid	66	127–129	MS [*m*/*z*, %]: 419 (M + 1, 27.3). FT-IR (cm^{-1}, KBr): v 758.85 (p-sub), 1053.90, 1255.92 (C—O—C), 1474.43, 1611.82 (C═C), 1670.42 (C═O), 1729.54 (C═O), 2936.77 (C—H), 3056.06 (Ar—C—H), 3274.30 (O—H), 3469.42 (N—H). ^{1}H NMR (400 MHz, DMSO d_6, ppm): 2. 27 (s, 3H, C—H), 4. 88 (s, 1H, C—H), 5. 22 (s, 1H, O—H), 6. 78 (s, 2H, N—H), 7. 15–7. 65 (m, 8H, Ar), 8. 17 (d, 2H, H—C═C—H), 9. 56 (s, H, O—H). ^{13}C NMR (100 MHz, DMSO d_6, ppm): 43.3 (C—CH), 17.95 (Me), 115.2–154.3 (Ar—C), 142.6 (C═C), 166.7 (C—O), 150.1, 162.2, 157.2, 193.5 (C═O).
6	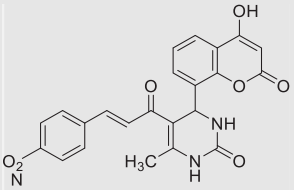 $C_{23}H_{18}N_2O_6$	Brown solid	54	173–174	MS [*m*/*z*, %]: 448 (M + 1, 27.3). FT-IR (cm^{-1}, KBr): v 758.70 (p-sub), 1058.90, 1282.41 (C—O—C), 1345.72, 1522.95 (NO_2), 1474.91, 1602.80 (C═C), 1692.09 (C═O), 2927.05 (C—H), 3081.44 (Ar—C—H), 3113.81 (O—H), 3479.91 (N—H). ^{1}H NMR (400 MHz, DMSO d_6, ppm): 2. 42 (s, 3H, C—H), 4. 75 (s, 1H, C—H), 7. 05 (s, 2H, N—H), 7. 34–7. 78 (m, 8H, Ar), 8. 30 (d, 2H, H—C═C—H), 9. 05 (s, 1H, O—H). ^{13}C NMR (100 MHz, DMSO d_6, ppm): 45.6 (C—C—H), 20.13 (Me), 95.2–154.2 (Ar—C), 142.3 (C═C), 166.4 (C—O), 150.5, 162.4, 193.6 (C═O).
7	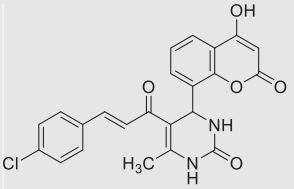 $C_{23}H_{17}ClN_2O_5$	Golden yellow solid	78	182–184	MS [*m*/*z*, %]: 438 (M + 2, 32.1). FT-IR (cm^{-1}, KBr): v 758.80 (p-sub), 1133.74 (C—Cl), 1057.02, 1281.65 (C—O—C), 1474.92, 1601.50 (C═C), 1672.64 (C═O), 1732.87 (C═O), 2928.97 (C—H), 3062.82 (C—H Ar), 3238.59 (O—H), 3438.02 (N—H). ^{1}H NMR (400 MHz, DMSO d_6, ppm): 2. 49 (s, 3H, C—H), 4. 92 (s, 1H, C—H), 7. 03–7. 75 (m, 12H, Ar), 9. 09 (s, 1H, O—H). ^{13}C NMR (100 MHz, DMSO d_6, ppm): 43.2 (C—C—H), 20.4 (Me), 92.1–154.4 (Ar—C), 143.5 (C═C), 166.7 (C—O), 150.1, 162.8, 193.3 (C═O).
8	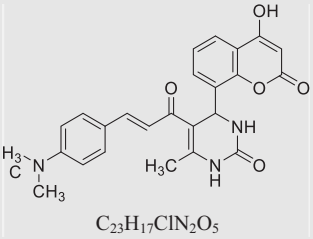 $C_{23}H_{17}ClN_2O_5$	Dark brown solid	58	144–146	MS [*m*/*z*, %]: 446 (M + 1, 27.5). FT-IR (cm^{-1}, KBr): v 765.60 (p-sub), 1058.20, 1268.19 (C—O—C), 1472.76, 1608.99 (C═C), 1713.23 (C═O), 2925.02 (C—H), 3032.82 (C—H Ar), 3225.82 (O—H), 3402.82 (N—H). ^{1}H NMR (400 MHz, DMSO d_6, ppm): 2. 47 (s, 3H, C—H), 3. 10 (s, 6H, C—H), 5. 05 (s, 1H, C H), 6. 50 (s, 2H, N—H), 7. 25–7. 73 (m, 8H, Ar), 7. 95 (d, 2H, H—C═C—H), 9. 05 (s, 1H, O—H). ^{13}C NMR (100 MHz, DMSO d_6, ppm): 45.1 (C—C—H), 40.2 (N—C—H), 20.7 (Me), 92.5–154.4 (Ar—C—N), 142.1 (C═C), 166.3 (C—O), 150.4, 162.2, 193.6 (C═O).
9		Orange solid	68	155–157	MS [*m*/*z*, %]: 419 (M + 1, 25.3). FT-IR (KBr, cm^{-1}): v 757.02 (o-sub), 1056.19, 1246.19 (C—O—C), 1475.03, 1601.37 (C═C), 1667.34 (C═O), 2928.10 (C—H), 3062.02 (C—H Ar), 3234.69 (O—H),

(*continued on next page*)

Table 1 (*continued*)

Compound Code	Chemical Structure/Formula	Appearance	% Yield	Melting Point (°C)	Spectral data
	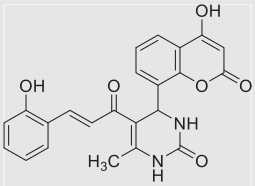 $C_{23}H_{17}ClN_2O_5$				3452.63 (N—H). ^{1}H NMR (400 MHz, DMSO d_6, ppm): 2. 38 (s, 3H, C—H), 4. 74 (s, 1H, C—H), 5. 27 (s, 1H, O—H), 6. 72 (s, 2H, N—H), 7. 20–7. 84 (m, 8-H, Ar), 8. 21 (d, 2H, H—C═C—H), 9. 51 (s, 1H, O—H). ^{13}C NMR (100 MHz, DMSO d_6, ppm): 43.4 (C—H), 20.2 (Me), 91.3–148.4 (Ar—C), 152.4 (C═C), 154.6 (Ar—C—N), 157.4, 166.7 (C—O), 150.7, 162.8, 193.1 (C═O).
10	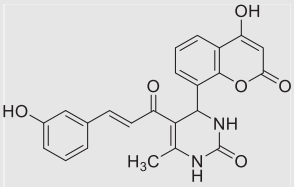 $C_{23}H_{18}N_2O_6$	Yellow solid	53	136–138	MS [*m*/*z*, %]: 419 (M + 1, 25.3). FT-IR (KBr, cm^{-1}): v 757.58 (m-sub), 1058.43, 1256.20 (C—O—C), 1474.96, 1601.00 (C═C), 1672.46 (C═O), 1730.83 (C═O), 2930.94 (C—H), 3046.83 (C—H Ar), 3237.16 (O—H), 3458.30 (N—H). ^{1}H NMR (400 MHz, DMSO d_6, ppm): 2. 44 (s, 3H, C—H), 5. 03 (s, 1H, C—H), 5. 37 (s, 1H, O—H), 6. 78 (s, 2H, N—H), 7. 15–7. 77 (m, 8H, Ar), 8. 05 (d, 2H, H—C═C—H), 9. 08 (s, 1H, O—H). ^{13}C NMR (100 MHz, DMSO d_6, ppm): 45.2 (C—H), 20.4 (Me), 91.2–148.2 (Ar—C), 142.5 (C═C), 154.3 (Ar—C—N), 158.2, 166.3 (C—O), 150.2, 162.3, 193.4 (C═O).
11	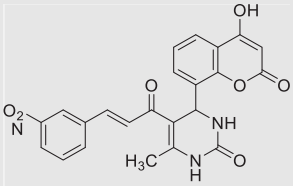 $C_{23}H_{17}N_3O_7$	Greenish white solid	59	103–105	MS [*m*/*z*, %]: 448 (M + 1, 25.3). FT-IR (cm^{-1}, KBr): v 753.98 (m-sub), 1035.69, 1235.69 (C—O—C), 1282.52, 1489.11 (nitro), 1474.83, 1609.12 (C═C), 1673.54 (C═O), 2926.11 (C—H), 3049.26 (C—H Ar), 3238.56 (O—H), 3385.87 (N—H), ^{1}H NMR (400 MHz, DMSO d_6, ppm): 2. 38 (s, 3H, C—H), 4. 89 (s, 1H, C—H), 6. 49 (s, 2H, N—H), 7. 13–7. 85 (m, 8H, Ar), 8. 52 (d, 2H, H—C═C—H), 9. 81 (s, 1H, O—H). ^{13}C NMR (100 MHz, DMSO d_6, ppm): 41.9 (C—C—H) 17.8 (Me), 92.4–148.5 (Ar—C), 142.7 (C═C), 147.5, 154.3 (Ar—C—N), 166.7 (C—O), 150.6, 162.1, 193.2 (C═O).
12	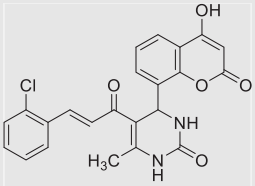 $C_{23}H_{17}ClN_2O_5$	Brown solid	57	106–107	MS [*m*/*z*, %]: 438 (M + 2, 32.5). FT-IR (cm^{-1}, KBr): v 757.55 (o-sub), 1129.44 (C—Cl), 1071.50, 1235.69 (C—O—C), 1476.30, 1610.40 (C═C), 1673.89 (C═O), 2926.15 (C—H), 3058.04 (C—H Ar), 3167.68 (O—H), 3379.99 (N—H). ^{1}H NMR (400 MHz, DMSO d_6, ppm): 2. 41 (s, 3H, C—H), 4. 95 (s, 1H, C—H), 6. 81 (s, 2H, N—H), 6. 81–7. 45 (m, 8H, Ar), 8. 20 (d, 2H, H—C═C—H), 9. 03 (s, 1H, O—H). ^{13}C NMR (100 MHz, DMSO d_6, ppm): 42.3 (C—C—H), 20.2 (Me), 91.7–148.1 (Ar—C), 122.2 (C═C), 134.5 (C—Cl), 154.3 (Ar—C—N), 166.3 (C—O), 150.2, 162.6, 193.2 (C═O).
13	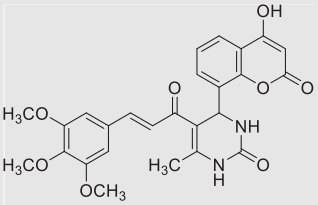 $C_{26}H_{24}N_2O_8$	Brick red solid	65	153–155	MS [*m*/*z*, %]: 493 (M + 1, 28.7). FT-IR (cm^{-1}, KBr): v 645.72, 758.51 (3,4,5-sub), 1055.43, 1281.26 (C—O—C), 1601.22 (C═C), 1675.62 (C═O), 2839.95 (C—H), 2939.21 (C—H Ar), 3234.51 (O—H), 3414.49 (N—H). ^{1}H NMR (400 MHz, DMSO d_6, ppm): 2. 47 (s, 3H, C—H), 3. 91 (s, 9H, C—H), 4. 78 (s, 1H, C—H), 6. 75 (s, 2H, N—H), 7. 22–7. 68 (m, 6H, Ar), 8. 10 (s, 2H, H—C═C—H), 9. 08 (s, 1H, O—H). ^{13}C NMR (100 MHz, DMSO d_6, ppm): 40.4 (C—H), 20.5 (Me), 56.5, 60.7 (O—CH_3), 92.4–148.5 (Ar—C), 142.5 (C═C), 154.5 (Ar—C—N), 138.5, 153.1, 166.3 (C—O), 150.7, 162.4, 193.6 (C═O).

Table 2 Physical properties and spectral data of hybrids ***14–26.***

Compound Code	Chemical Structure/Formula	Appearance	% Yield	Melting Point (°C)	Spectral data
TUD	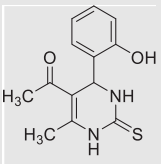 $C_{13}H_{14}N_2O_2S$	Cream colour crystals	74	173–175	MS [*m*/*z*, %]: 263 (M + 1, 12). FT-IR (KBr, cm^{-1}): v 1275.21 (C—O), 1472.97, 1602.84 (C═C), 1671.10 (C═O), 2925.07 (C—H), 3021.42 (Ar—C—H), 3420.82 (O—H), 3248.73 (N—H). ^{1}H NMR (400 MHz, DMSO d_6, ppm): 1. 35 (s, 3H, C—H), 2. 03 (s, 2H, N—H, Ar), 2. 82 (s, 3H, C—H—C═O), 4. 96 (s, 1H, C—H), 5. 21 (s, 1H, O—H), 6. 56–6. 95 (m, 4H, Ar). ^{13}C NMR (100 MHz, DMSO d_6, ppm): 42.5 (C—H, Ar), 27.2 (Me), 17.8 (Me), 104.6–128.6 (Ar—C), 154. 6 (C—O—H), 158. 1 (C—N), 174. 5 (C═S), 196. 3 (C═O).
CTUD	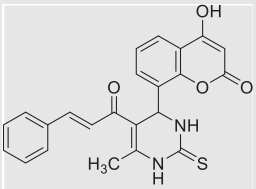 $C_{23}H_{18}N_2O_4S$	Red crystals	81	111–113	MS [*m*/*z*, %]: 331 (M + 1, 9). FT-IR (cm^{-1}, KBr): v 1475.26 (C═C), 1612.04 (C—O), 1665.93 (C═O), 2930.11 (C—H), 3016.77 (C—H Ar), 3248.29 (N—H), 3418.82 (O—H). ^{1}H NMR (400 MHz, DMSO d_6, ppm): 1. 26 (s, 3H, C—H), 2. 08 (s, 2H, N—H, Ar), 2. 62 (s, 3H, C—H—C═O), 4. 74 (s, 1H, C—H), 6. 76–7. 10 (m, 4H, Ar), 9. 35 (s, 1H, O—H). ^{13}C NMR (100 MHz, DMSO d_6, ppm): 43.7 (C—H, Ar), 27.6 (Me), 15.4 (Me), 91.6–148.2 (Ar—C), 158. 4 (CN), 166. 2 (C—O), 174. 1 (C═S), 160. 5, 196. 7 (C═O).
14	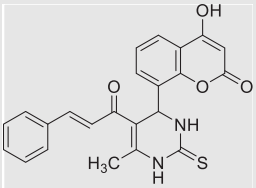 $C_{23}H_{18}N_2O_4S$	Yellow solid	69	106–108	MS [*m*/*z*, %]: 419 (M + 1, 11). FT-IR (cm^{-1}, KBr): v 1039.60, 1232.87 (C—O), 1490.49, 1608.91 (C═C), 1671.08 (C═O), 2850.79 (C—H), 2919.91 (Ar—C—H), 3347.96 (N—H), 3472.96 (O—H). ^{1}H NMR (400 MHz, DMSO d_6, ppm): 2. 42 (s, 3H, C—H), 4. 85 (s, 1H, C—H), 6. 35 (s, 2H, N—H), 6. 37–7. 33 (m, 9H, Ar), 7. 89 (d, 2H, C═C), 9. 12 (s, 1H, O—H). ^{13}C NMR (100 MHz, DMSO d_6, ppm): 43.7 (C—C—H), 17.2 (Me), 91.5–148.5 (Ar—C), 166.1 (C—O—H), 167.8 (C—N), 174.4 (C═S), 160.6, 193.8 (C═O).
15	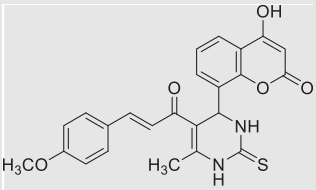 $C_{24}H_{20}N_2O_5S$	Dark red solid	61	146–148	MS [*m*/*z*, %]: 449 (M + 1, 10). FT-IR (cm^{-1}, KBr): v 759.79 (o-sub), 1050.02, 1287.92 (C—O), 1425.17 (C═C), 3424.04 (O—H), 1602.27 (C═C), 1682.31 (C═O), 2948.84 (C—H), 3055.15 (Ar—C—H), 3318.93 (N—H). ^{1}H NMR (400 MHz, DMSO d_6, ppm): 2. 38 (s, 3H, C—H), 3. 14 (s, 3H, C—H), 4. 66 (s, 1H, C—H), 6. 11 (2H, N—H), 6. 69–7. 21 (m, 8H, Ar), 7. 61 (d, 2H, C═C), 9.58 (s, 1H, O—H). ^{13}C NMR (100 MHz, DMSO d_6, ppm): 55.4 (Me), 42.9 (C—C—H), 15.8 (Me), 91.2–148.5 (Ar—C), 152. 5 (C═C), 158. 2 (C—OCH_3), 166. 8 (C—O—H), 167. 4 (C—N), 174. 1 (C═S), 160.7,193.2 (C═O).
16	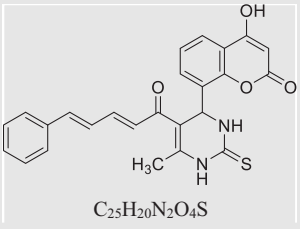 $C_{25}H_{20}N_2O_4S$	Yellow solid	58	142–144	MS [*m*/*z*, %]: 445 (M + 1, 8). FT-IR (cm^{-1}, KBr): v 753.87 (Ar), 1411.10 (C═C), 1688.83 (C═O), 2893.03 (C—H), 3013.90 (Ar—C—H), 3218.17 (N—H), 3415.38 (O—H). ^{1}H NMR (400 MHz, DMSO d_6, ppm): 2. 56 (s, 3H, C—H), 4. 85 (s, 1H, C—H), 6. 15 (s, 2H, N—H), 6. 91–7. 35 (m, 9H, Ar), 7. 55 (d, 2H, C═C), 9. 47 (s, 1H, O—H). ^{13}C NMR (100 MHz, DMSO d_6, ppm): 43.7 (C—C—H), 17.3 (Me), 91.8–135.4 (Ar—C), 131. 5, 151. 5 (C═C), 166. 2 (C—O), 167. 9 (C—N), 174. 7 (C═S), 160.3, 193.4 (C═O).
17		Green solid	66	152–154	MS [*m*/*z*, %]: 464 (M + 1, 8). FT-IR (cm^{-1}, KBr): v 783.91 (p-sub), 1045.88, 1282.05 (C—O), 1445.24 (C═C), 1382.15, 1535.04 (NO_2), 1684.37 (C═O), 2938.22 (C—H), 3019.29 (Ar—C—H), 3284.49

(*continued on next page*)

Table 2 (*continued*)

Compound Code	Chemical Structure/Formula	Appearance	% Yield	Melting Point (°C)	Spectral data
	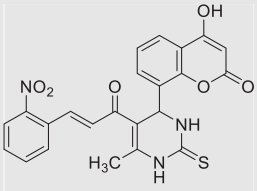 $C_{23}H_{17}N_3O_6S$				(N—H), 3462.82 (O—H). ^{1}H NMR (400 MHz, DMSO d_6, ppm): 2. 29 (s, 3H, C—H), 4. 85 (s, 1H, C—H), 6. 06 (s, 2H, N—H), 6. 80–7. 38 (m, 8H, Ar), 7. 64 (d, 2H, C═C), 9 0.47 (s, 1H, O—H). ^{13}C NMR (100 MHz, DMSO d_6, ppm): 43.8 (C—C—H), 15.7 (Me), 91.6–148.6 (Ar—C), 153.4 (C═C), 166. 7 (C—O), 167. 4 (C—N), 160.3, 193.5 (C═O).
18	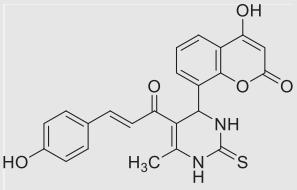 $C_{23}H_{18}N_2O_5S$	Reddish Brown solid	69	176–178	MS [*m*/*z*, %]: 435 (M + 1, 12). FT-IR (cm^{-1}, KBr): v 752.11 (o-sub), 1055.10, 1282.84 (C—O), 1605.72 (C═C), 1679.04 (C═O), 2942.70 (C—H), 3021.29 (Ar—C—H), 3295.44 (N—H), 3437.38 (O—H). ^{1}H NMR (400 MHz, DMSO d_6, ppm): 2. 37 (s, 3H, C—H), 4. 77 (s, 1H, C—H, Ar), 5. 26 (s, 1H, O—H), 6. 02 (s, 2H, N—H), 6. 55–7. 25 (m, 8H, Ar), 7. 60 (d, 2H, C—H═C—H), 9. 58 (s, 1H, O—H). ^{13}C NMR (100 MHz, DMSO d_6, ppm): 45.6 (C—C—H), 18. 36 (Me), 91.3–148.4 (Ar—C), 152.2 (C═C), 157.8, 166.1 (C—O—H), 167.4 (C—N), 174.7 (C═S), 161.7, 193.5 (C═O).
19	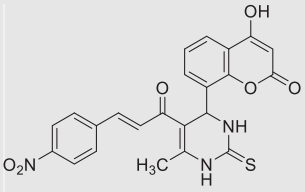 $C_{23}H_{17}N_3O_6S$	Brown solid	63	255–257	MS [*m*/*z*, %]: 464 (M + 1, 8). FT-IR (cm^{-1}, KBr): v 762.99 (o-sub), 1289.94 (C—O), 1326.19, 1532.73 (NO_2), 1603.28 (C═C), 1675.13 (C═O), 2915.27 (C—H), 3048.28 (Ar—C—H), 3297.36 (N—H), 3454.49 (O—H). ^{1}H NMR (400 MHz, DMSO d_6, ppm): 2. 42 (s, 3H, C—H), 4. 91 (s, 1H, C—H), 6. 10 (s, 2H, N—H), 6. 80–7. 74 (m, 8H, Ar), 8. 20 (d, 2H, C═C), 9. 74 (s, 1H, O—H). ^{13}C NMR (100 MHz, DMSO d_6, ppm): 44.7 (C—C—H), 17.8 (Me), 91.8–148.3, (Ar—C), 152. 6 (C═C), 166. 6 (C—O), 168. 4 (C—N), 160. 1, 193. 2 (C═O).
20	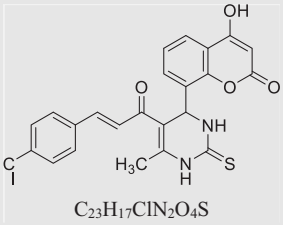 $C_{23}H_{17}ClN_2O_4S$	Golden yellow solid	57	170–172	MS [*m*/*z*, %]: 453 (M + 1, 12). FT-IR (cm^{-1}, KBr): v 751.23 (o-sub), 1289.48 (C—O), 1614.83 (C═C), 1682.71 (C═O), 2942.93 (C—H), 3019.84 (Ar—C—H), 3265.52 (N—H), 3405.40 (O—H). ^{1}H NMR (400 MHz, DMSO d_6, ppm): 2. 39 (s, 3H, C—H), 4. 80 (s, 1H, C—H), 6. 16 (s, 2H, N—H), 6. 80–7. 30 (m, 8H, Ar), 7. 74 (d, 2H, C—H═C—H), 9. 31 (s, 1H, O—H). ^{13}C NMR (100 MHz, DMSO d_6, ppm): 40.6 (C—C—H), 16.3 (Me), 91.6–133.8, (Ar—C), 152.7 (C—H═C—H), 166. 4 (C—O), 167. 2 (C—N), 174. 2 (C═S), 160.4, 193.3 (C═O).
21	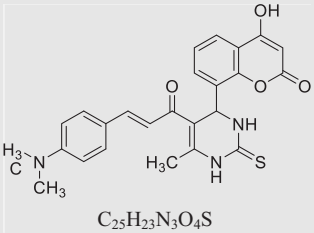 $C_{25}H_{23}N_3O_4S$	Dark brown solid	74	159–161	MS [*m*/*z*, %]: 442 (M + 1, 9). FT-IR (cm^{-1}, KBr): v 757.62 (p-sub), 1042.07, 1233.48 (C—O), 1599.36 (C═C), 1649.61 (C═O), 2850.99 (C—H), 2920.07 (Ar—C—H), 3389.55 (N—H), 3416.42 (O—H). ^{1}H NMR (400 MHz, DMSO d_6, ppm): 2. 45 (s, 3H, C—H), 2. 94 (s, 6H, C—H), 5. 10 (s, 1H, C—H), 6. 35 (s, 2H, N—H), 6. 55–7. 15 (m, 8H, Ar), 7. 70 (d, 2H, C—H═C—H), 9. 11 (s, 1H, O—H). ^{13}C NMR (100 MHz, DMSO d_6, ppm): 45.1 (C—C—H), 40.2 (N—C—H), 20.7 (Me), 92.5–128.7 (Ar—C), 148. 4, 167.2 (Ar—C—N), 166. 6 (C—O), 152. 7 (C═C), 174. 2 (C═S), 160. 8, 193. 3 (C═O).
22		Orange solid	58	176–178	MS [*m*/*z*, %]: 435 (M + 1, 11). FT-IR (cm^{-1}, KBr,): v 758.14 (o-sub), 1232.35 (C—O), 1610.84 (C═C), 1688.21 (C═O), 2851.59 (C—H), 2922.28 (C—H Ar), 3251.62 (N—H), 3437.33 (O—H),

Table 2 (*continued*)

Compound Code	Chemical Structure/Formula	Appearance	% Yield	Melting Point (°C)	Spectral data
	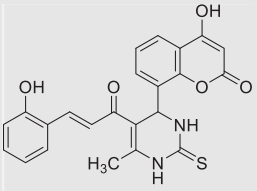 $C_{23}H_{18}N_2O_5S$				^{1}H NMR (400 MHz, DMSO d_6, ppm): 2. 53 (s, 3H, C—H), 4. 91 (s, H, C—H), 5. 24 (s, 1H, O—H), 6. 42 (s, 2H, N—H), 6. 55–7. 20 (m, 8H, Ar), 7. 39 (d, 2H, C—H═C—H), 9. 10 (s, 1H, O—H). ^{13}C NMR (100 MHz, DMSO d_6, ppm): 45.1 (C—C—H), 16.8 (Me), 91.7–148.1 (Ar—C), 158. 3, 162. 7 (Ar—C—O), 167. 3 (C—N), 174. 3 (C═S), 160. 3, 193. 4 (C═O).
23	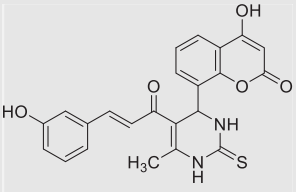 $C_{23}H_{18}N_2O_5S$	Yellow solid	65	175–177	MS [*m*/*z*, %]: 435 (M + 1, 9). FT-IR (cm^{-1}, KBr): v 754.42 (m-sub), 1275.39 (C—O), 1472.50 (C═C), 1692.77 (C═O), 2892.27 (C—H), 3011.25 (Ar—C—H), 3158.86 (N—H), 3437.39 (O—H), ^{1}H NMR (400 MHz, DMSO d_6, ppm): 2. 30 (s, 3H, C—H), 4. 71 (s, H, C—H), 5. 38 (s, 1H, O—H), 6. 14 (s, 2H, N—H), 6. 65–7. 10 (m, 8H, Ar), 7. 69 (d, 2H, C—H═C—H), 9. 52 (s, 1H, O—H). ^{13}C NMR (100 MHz, DMSO d_6, ppm): 42.8 (C—C—H), 18.7 (Me), 91.5–148.6 (Ar—C), 152. 8 (CH═CH), 158. 7, 166. 3 (C—O), 167. 8 (C—N), 174. 5 (C═S), 160.6, 193.4 (C═O).
24	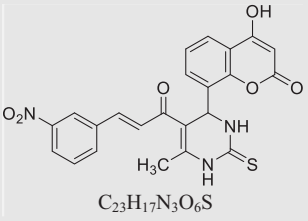 $C_{23}H_{17}N_3O_6S$	Greenish white solid	59	149–151	MS [*m*/*z*, %]: 464 (M + 1, 11). FT-IR (cm^{-1}, KBr): v 757.17 (m-sub), 1282.24 (C—O), 1344.81 (NO_2), 1489.14 (C═C), 1688.53 (C═O), 2944.49 (C—H), 3036.38 (Ar—C—H), 3264.74 (N—H), 3399.33 (O—H). ^{1}H NMR (400 MHz, DMSO d_6, ppm): 2. 47 (s, 3H, C—H), 4. 72 (s, 1H, C—H), 6. 17 (s, 2H, N—H), 6. 80–7. 62 (m, 8H, Ar), 8. 30 (d, 2H, C═C), 9. 88 (s, 1H, O—H). ^{13}C NMR (100 MHz, DMSO d_6, ppm): 43.6 (C—C—H), 16.3 (Me), 91.8–148.2 (Ar—C), 147.5, 152.6 (C—H═C—H), 165. 3 (C—O), 167. 8 (C—N), 174. 7 (C═S), 160.2, 193.2 (C═O).
25	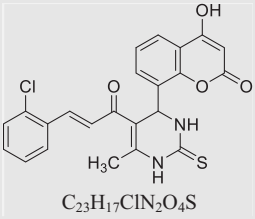 $C_{23}H_{17}ClN_2O_4S$	Brown solid	65	137–139	MS [*m*/*z*, %]: 453 (M + 2, 14). FT-IR (cm^{-1}, KBr): v 752.55 (p-sub), 1284.41 (C—O), 1602.20 (C═C), 1688.85 (C═O), 2938.95 (C—H), 3046.38 (Ar—C—H Ar), 3245.46 (N—H), 3414.29 (O—H). ^{1}H NMR (400 MHz, DMSO d_6, ppm): 2. 35 (s, 3H, C—H), 4. 68 (s, 1H, C—H), 6. 11 (s, 2H, N—H), 6. 85–8. 30 (m, 8H, Ar), 7. 92 (d, 2H, C—H═C—H), 9. 82 (s, 1H, O—H). ^{13}C NMR (100 MHz, DMSO d_6, ppm): 41.7 (C—C—H), 18.3 (Me), 91.2–133.6, (Ar—C), 152.7 (C—H═C—H), 166. 6 (C—O), 167. 8 (C—N) 174. 8 (C═S), 160.5, 193.5 (C═O)
26	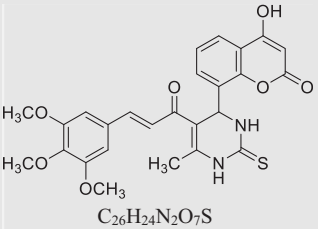 $C_{26}H_{24}N_2O_7S$	Brick red solid	74	216–218	MS [*m*/*z*, %]: 509 (M + 1, 14). FT-IR (cm^{-1}, KBr): v 646.13, 760.20 (3,4,5-sub), 1040.86, 1233.34 (C—O), 1457.47, 1597.22 (C═C), 1696.30 (C═O), 2840.24 (C—H), 2938.13 (Ar—C—H), 3291.61 (N—H), 3426.02 (O—H). ^{1}H NMR (400 MHz, DMSO d_6, ppm): 2. 45 (s, 3H, C—H), 3. 75 (s, 9H, C—H), 4. 93 (s, 1H, C—H), 6. 32 (s, 2H, N—H), 6. 60–7. 10 (m, 6H, Ar), 7. 75 (d, 2H, C—H═C—H), 9. 29 (s, 1H, O—H). ^{13}C NMR (100 MHz, DMSO d_6, ppm): 56.8, (OMe), 42.8 (C—C—H), 16.3 (Me), 91.7–148.2 (Ar—C), 150. 5 (C—OMe), 152. 4 (C—H═C—H), 166. 1 (C—O), 167. 5 (C—N), 174. 8 (C═S), 160. 3, 193. 2 (C═O).

Table 3 Antimicrobial activity of coumarin clubbed chalcones against selected bacterial and fungal strains.

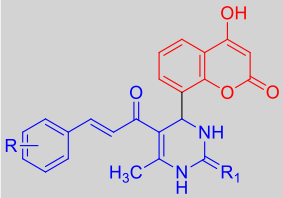

1-13 = R_1= O
14-26 = R_1= S

S. No.	Compound	MIC (μM)			S. No.	Compound	MIC (μM)		
		Sa	*Ec*	*An*			*Sa*	*Ec*	*An*
1	**1**	**10.05**	**8.04**	**10.05**	15	**14**	R	R	R
2	**2**	21.60	17.28	R	16	**15**	R	33.60	R
3	**3**	21.40	32.10	R	17	**16**	R	44.40	R
4	**4**	33.52	R	R	18	**17**	R	R	R
5	**5**	20.90	31.25	R	19	**18**	43.40	R	R
6	**6**	26.82	44.70	22.35	20	**19**	R	R	R
7	**7**	**17.44**	**13.08**	**10.90**	21	**20**	R	R	R
8	**8**	22.25	R	R	22	**21**	R	R	R
9	**9**	16.72	20.90	31.35	23	**22**	21.50	21.50	R
10	**10**	R	R	R	24	**23**	R	R	R
11	**11**	31.29	44.70	R	25	**24**	34.72	R	R
12	**12**	R	R	R	26	**25**	R	R	R
13	**13**	24.60	49.2	24.60	27	**26**	R	R	R
14	Ciprofloxacin	0.24	0.06	-	28	Fluconazole	-	-	0.15

Sa: *Staphylococcus aureus*; *Ec*: *Escherichia coli*; *An*: *Aspergillus niger*; R = Resistance.

and sofalcone (Fig. 1) that are used as choleretic and antiulcer agents (Aksoz and Ertan, 2013, Sahu et.al., 2012, Shigeru et. al.,1991). Additionally, clinical trials data indicated that hesperidin trimethylchalcone and hesperidin methylchalcone screened for branch or trunk varicosis and chronic venous lymphatic insufficiency respectively were biologically effective due to their ability to reach required concentrations in plasma, reducing the symptoms and good acceptance by the physiological system (Liu et.al., 2016, Beltramino et.al., 2000, Guan et. al., 2014).

Many scientists synthesized and screened various coumarin hybrids as well as the chalcone hybrids with potential bioactivities. Molecular hybrids of coumarins and chalcones possess excellent antibacterial (Feng et.al., 2020, Osman et.al.,2018, Sanad and Mekky, 2020, Kraljević et.al., 2016, Sahoo et al., 2021, Lipeeva et.al.,2019, Vazquez-Rodriguez et.al., 2015, Sashidhara et.al., 2015, Shaik et.al., 2017, Wang et al., 2019b, Sribalan et al., 2016), antifungal (Zhang et al., 2021, Yang and Liang, 2021, Patel et al., 2017, Sharma and Katiyar, 2019, Prusty and Kumar, 2020; Mellado et al., 2020, Singh et al., 2018, Shaik et al., 2020b, Kant et al., 2016, Lagu et al., 2020, Akkulu Naidu and Rajendra Prasad, 2018), antioxidant (Matos et al., 2015, Nagamallu et al., 2016, Karina et al., 2018, Shi et al., 2020, Şenocak et al., 2018, Aneja et al., 2018, Jakovljević et al., 2018, Xue et al., 2018, Latif et al., 2020, Arif et al., 2020, Kostopoulou et al., 2020) and anticancer activities (Zhang and Xu, 2019, Kurt et al., 2020, Kamath et al., 2015, Xu et al., 2019, Song et al., 2020, Goud et al., 2019, Gao et al., 2020, Park et al., 2018, Wang et al., 2019a, Mirzaei et al., 2020, Djemoui et al., 2020) etc. Coumarins and chalcones comprise antioxidant activity due to their ability to influence the formation and scavenging of reactive oxygen species (ROS) (Fylaktakidou et al., 2004, Sökmen and Khan, 2016). Similarly, a variety of mechanisms are responsible for the antibacterial and antifungal activities of coumarins and chalcones (Qin et al., 2020, Srikrishna et al., 2018, Hu et al., 2018, Dan and Dai, 2020, Farhadi et al., 2018, Xu et al., 2019, Wei et al., 2016). Coumarin containing hybrids like clorobiocin, coumermycin A1 as well as novobiocin are already employed clinically to treat different bacterial infections. Hence, it is possible to link coumarin moiety with another antimicrobial pharmacophore like chalcone via the molecular hybridization strategy to yield novel drugs against infectious diseases. Coumarins and chalcones can be conveniently synthesized in the laboratory through Pechmann and Claisen-Schmidt condensation reactions (Gaudino et al., 2016, Shaik et al., 2019, Chavan et al., 2017, Vijaya Bhargavi et.al., 2017).

Bearing in mind the synthetic feasibility and promising bioactivities of hybrids derived from coumarins and chalcones, in the present investigation we prepared (Scheme 1) and screened the antimicrobial and antioxidant properties of novel coumarin-clubbed chalcone derivatives (Fig. 2).

2. Materials and methods

2.1. General

The chemicals and reagents employed for the synthesis were purchased from local suppliers and the melting points of the prepared compounds were determined using Dalal melting point apparatus in open capillary tubes. FT-IR spectra were scanned by KBr-Pellet method. ^{1}H NMR and ^{13}C NMR spectra and mass spectra were recorder at Laila Impex, Vijayawada, Andhra Pradesh, India by using a Bruker-NMR Spectrometer 400 MHz and Shimadzu GCMS QP 5000 mass spectrometers respectively. Other chemicals were of commercial grade and used without any purification further. The reactions were monitored by thin-layer chromatography (TLC) on silica gel F_{254} aluminium TLC plates (Merck, Germany) using ethyl acetate (EtOAc)-hexane mixture as mobile phase. The spots on the TLC plate were visualized using iodine vapours and UV lamp.

2.2. Experimental

*2.2.1. Synthesis of 5-Acetyl-4-(2-hydroxyphenyl)-6-methyl-3,4-dihydropyrimidin-2(1H)-one (**UD**)*

2-Hydroxybenzaldehyde (1 mmol), 1.1 mmol of pentane-2,4-dione and 1.3 mmol of urea were refluxed and stirred in 100 mL round bottom flask (RBF) at 80 ^{0}C in the presence of 0.5 mmol of citric acid as catalyst. After the end of the reaction (that is monitored through TLC 30% EtOAc: Hexane mixture), the reaction mixture was charged with 100 mL of cold water and stirred for another 10 min. This led to the formation of a precipitate which was further filtered and thoroughly washed with distilled water and dried in vacuum to get the crude solid that was purified further by recrystallization using ethanol (Yield, 85%) [Hajelsiddig and Saeed, 2015].

*2.2.2. Synthesis 5-Acetyl-4-(4-hydroxy-2-oxo-2H-chromen-8-yl)-6-methyl-3,4-dihydropyrimidin-2(1H)-one (**CUD**)*

To a mixture of 5-Acetyl-4-(2-hydroxyphenyl)-6-methyl-3,4-dihydropyrimidin-2(1H)-one (0.1 mol) and malonic acid (0.1 mol), 40 mL of phosphorus oxychloride and 30 g of anhydrous zinc chloride (preheated to 60–70 °C) were added. The above mixture was heated for 20 h at 70 °C and after the completion of the reaction that was monitored by TLC (40% EtOAc-Hexane mixture), 50 mL of ice-cold water was added to the reaction mixture to form a precipitate. The formed precipitate was washed thoroughly with cold water and then filtered. The solid thus obtained was treated with 10% sodium carbonate solution and filtered and to the filtrate diluted hydrochloric acid was added to obtain crude product. The crude product was filtered, washed with water, dried and recrystallized using glacial acetic acid (Yield, 74%) [Potdar et al., 2005].

*2.2.3. General procedure for synthesis coumarin clubbed chalone derivatives (**1–13**)*

5-Acetyl-4-(4-hydroxy-2-oxo-2H-chromen-8-yl)-6-methyl-3,4-dihydropyrimidin-2(1H)-one (0.002 mol) and substituted aromatic aldehyde (0.002 mol) were dissolved in 6 mL of ethanol. Then, 3 mL of 40% KOH was added drop wise to the above solution and the reaction mixture was stirred for 30 h. The completion of the reaction was monitored by TLC (30% EtOAc-Hexane for most of the compounds. However, for compounds **5**, **9** and **13**, 40% EtOAc-Hexane was used whereas for compound 6, 20% EtOAc-Hexane was employed as mobile phase). The reaction mixture was added with crushed ice and the contents were neutralized with dil. HCl to obtain a precipitate. The crude solid formed was recrystallized using ethanol (95%) [Konidala et al., 2021; Lokesh et al., 2017; Shaik et al., 2015]. Physical properties and spectral data of hybrids ***1–13*** are displayed in Table 1.

*2.2.4. General procedure for synthesis of 1-(4-(2-Hydroxyphenyl)-6-methyl-2-thioxo-1,2,3,4-tetrahydropyrimidin-5-yl)ethanone (**TUD**)*

TUD was synthesized and purified employing the same protocol as described under the general procedure for the synthesis of UD except that thiourea is replaced with urea.

*2.2.5. General procedure for synthesis 8-(5-acetyl-6-methyl-2-thioxo-1,2,3,4-tetrahydropyrimidin-4-yl)-4-hydroxy-2H-chromen-2-one **(CTUD)***

CTUD was synthesized and purified employing the same protocol as described under the general procedure for the synthesis of CUD except that 1-(4-(2-Hydroxyphenyl)-6-methyl-2-thioxo-1,2,3,4-tetrahydropyrimidin-5-yl)ethanone was used replacing 5-Acetyl-4-(2-hydroxyphenyl)-6-methyl-3,4-dihydro pyrimidin-2(1H)-one.

*2.2.6. General procedure for synthesis coumarin clubbed chalone derivatives (**14–26**)*

The same protocol employed for the synthesis of compounds 1–13 is utilized for the synthesis of the target compounds 14–26. However, in this case, CTUD was used as a starting material in the place of CUD and the reactions were monitored by TLC employing 50% EtOAc-Hexane as mobile phase [Konidala et.al., 2020]. Physical properties and spectral data of hybrids ***14–26*** were given in Table 2.

2.3. In vitro Anti-microbial activity:

The *in vitro* antimicrobial testing was performed by Agar well diffusion method [Bauer et.al., 1966, Lagu et.al., 2019] against *Staphylococcus aureus* (NCIM 2122), *Escherichia coli* (NCIM 2137) and *Aspergillus niger* (NCIM 652). The zone of inhibition of target compounds was measured and compared with standard drugs including ciprofloxacin and fluconazole. The microbial strains were sub-cultured in presterilized nutrient agar and potato dextrose agar media for antibacterial and antifungal activity respectively. Then the pre-inoculated medium was aseptically transferred into sterilized Petri plates of 4-inch diameter. After the solidification of the medium, sterilized cork borer was used make a cup of 6 mm and labelled. The solutions of the standard compound in concentration of 10 µg/ml was prepared in DMSO where as the solutions of the test compounds were obtained by dissolving in DMSO and diluting to a dose level of 25, 50, 75 and 100 µg/ml. These concentrations were later added to the bore of Petri plates under sterilized conditions, and the plates were incubated for 48 h. DMSO was used as a negative control and found no

effect. The Zone of inhibition was determined and MIC values were calculated for each test compound along with standard. The results of antibacterial activity are tabulated in Table 3.

2.4. In vitro antioxidant activity

The percentage of antioxidant activity (AA%) of each substance was determined by DPPH free radical assay method. DPPH radical scavenging activity [Shaik et al., 2020a] of the samples was assessed by reacting with stable DPPH radical in an ethanol solution. The reaction mixture comprises 0.5 mL of sample, 3 mL of absolute ethanol and 0.3 mL of 0.5 mM DPPH radical solution in ethanol. The change in the color from deep violet to light yellow due to the reaction of DPPH with the target compound was read at 517 nm after 30 min of reaction using a UV–VIS spectrophotometer. The mixture of ethanol (3.3 mL) and sample (0.5 mL) serve as blank whereas the control solution was prepared by mixing ethanol (3.5 mL) and DPPH radical solution (0.3 mL). The scavenging activity percentage (AA%) was determined according to previously reported method [Mensor et al., 2021].

$$AA\% = 100 - \left[\frac{(\text{Absorbance of the sample} - \text{Absorbance of Control})}{\text{Absorbance of Control}}\right] \times 100$$

3. Results and discussion

3.1. Chemistry

The acid catalyzed Biginelli reaction of salicylaldehyde with pentane-2,4-dione and urea/thiourea afforded the dihydropyrimidine derivatives, UD and TUD in 85.41% and 74.38% yields respectively. The characteristic absorption bands for the secondary amino group N—H at wave numbers 3370 and 3248 cm^{-1} and singlet peaks in the ^1H NMR for methine (CH) proton at the chemical shifts 4.91 and 4.96 ppm confirmed the formation of UD and TUD. Further Pechmann condensation of UD and TUD with malonic acid, phosphorous oxychloride and zinc chloride formed CUD (72.45%) and CTUD (81.66%) in good yields. The mass spectrum of these two compounds showed M + 1 peak at *m/z* values 315 and 331 corresponding to their molecular weights. Additionally, the FT-IR, ^1H NMR, and ^{13}C NMR spectrum of all the compounds and the mass spectrum of UD and TUD showed characteristic bands and peaks and established the structures of UD, TUD, CUD and CTUD. The target coumarin clubbed chalcone hybrids (**1–13** and **14–26**) were then synthesized by the base catalyzed Claisen-Schmidt condensation of CUD and CTUD with a variety of aromatic aldehydes in the yields ranging from 54.32 to 74.25%. These compounds showed the characteristic absorption bands in their FT-IR spectrums corresponding to the —CH=CH— and —C=O functional groups of the ketovinyl fragment of chalcones. Additionally, these hybrids also displayed characteristic peaks in their ^1H and ^{13}C nuclear magnetic resonance spectra's and the molecular ion peaks at their respective *m/z* values as M + 1 and M + 2 peaks aided in dereplicating the structure of the proposed target compounds.

3.2. Antimicrobial activity

The antimicrobial screening data of the two series of compounds (**1–13 series** and **14–26 series**) is depicted in Table 3. Ciprofloxacin and Fluconazole were used as reference standard for the assay. In addition, between these two series compounds belonging to **1–13** series contain oxygen in the pyrimidine ring whereas the **14–26** series compounds possess sulfur atom. Among the two series, compounds belonging to **1–13** series possess considerable antimicrobial activity and the organisms showed resistance for majority of compounds in **14–26** compounds series. Overall, the MIC values of the compounds are in the range of 8–49 μM. In **1–13** series, it can be seen that compound **1** (MICs 8–10) and **7** (10–17 μM) containing unsubstituted phenyl and 4-chlorophenyl ring showed better antimicrobial activity over other compounds (Fig. 3). However, despite of changing the electronic properties of the phenyl ring, no improvement was observed in the MIC values against reference standard.

3.3. Antioxidant activity

The antioxidant activity (Table 2) indicated by the % scavenging activity of synthesized compounds (**1–13** and **14–26**) was determined by the DPPH assay method, data is depicted in Table 4. Ascorbic acid (AA) and Butylated hydroxytoluene (BHT) were used as reference standard. The compounds and the standards were evaluated at a test concentration of 100 μg/ml. The compounds belonging to **14–26** series showed better antioxidant activity the compounds belonging to **1–13**

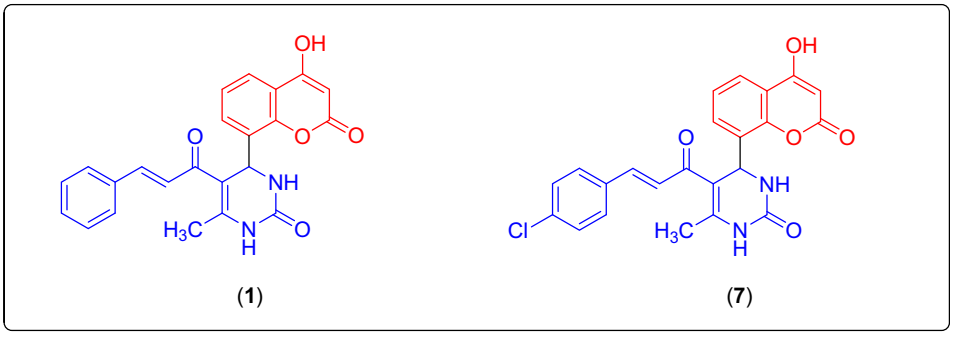

Fig. 3 Coumarin clubbed chalcone hybrids with considerable antimicrobial activity.

Table 4 Antioxidant activity of coumarin clubbed chalcone hybrids.

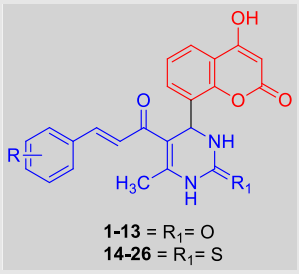

.

S. No	Compound Code	Concentration (µg/ml)	% Scavenging Activity	S. No	Compound Code	Concentration (µg/ml)	% Scavenging Activity
1	**1**	100	49.84±1.27	15	**14**	100	**75.22±0.58**
2	**2**	100	41.29±0.64	16	**15**	100	31.28±0.74
3	**3**	100	22.82±0.39	17	**16**	100	21.47±1.15
4	**4**	100	17.24±0.21	18	**17**	100	35.01±0.17
5	**5**	100	**66.21±1.04**	19	**18**	100	15.28±0.69
6	**6**	100	51.05±0.45	20	**19**	100	42.15±0.95
7	**7**	100	51.20±1.16	21	**20**	100	24.12±1.03
8	**8**	100	16.77±0.35	22	**21**	100	55.15±0.32
9	**9**	100	39.18±0.42	23	**22**	100	**77.92±1.28**
10	**10**	100	15.91±1.38	24	**23**	100	30.18±0.26
11	**11**	100	34.38±1.55	25	**24**	100	21.84±1.14
12	**12**	100	58.25±1.11	26	**25**	100	08.93±1.78
13	**13**	100	42.49±0.63	27	**26**	100	**71.32±0.92**
14	AA	100	81.21±3.63	28	BHT	100	70.05±1.58

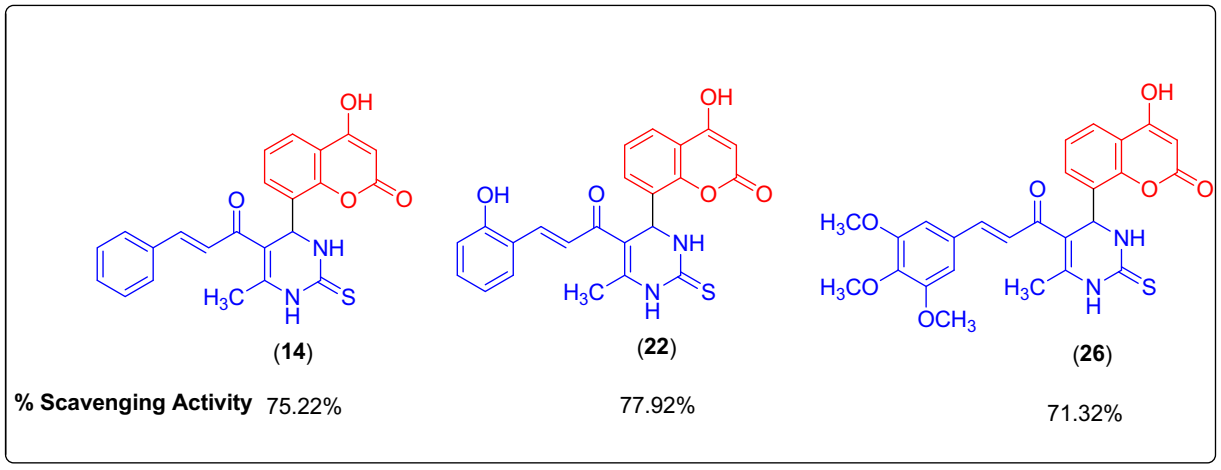

Fig. 4 Potential coumarin clubbed chalcone hybrids with antioxidant activity.

series. In **1**–**13** series, the best antioxidant activity was observed for compound **5** at 66%. The compounds **5**, **14**, **22** and **26** showed significant antioxidant activity with % scavenging activity in the range of 66.21–77.92 %. Among these, **14**, **22** and **26** containing unsubstituted phenyl ring and phenyl ring substituted with electron releasing 2-OH substitution and 3,4,5-trimethoxy substituents in chalcones with 3,4-dihydropyr imidine-2(1H)-thione moiety showed excellent antioxidant activity with 75.22%, 77.92% and 71.32% scavenging activity compared to BHT (Fig. 4). However, their activity was less but close to AA.

4. Conclusions

Two series (**1**–**13 series** and **14**–**26 series**) having a total of 26 new coumarin clubbed chalcone hybrids were synthesized, characterized and evaluated for their antimicrobial and antioxidant activities. The antimicrobial screening of all the synthesized compounds was done by *in-vitro* well diffusion method against Gram + ve, Gram -ve, and fungal strains, the results concluded that the compounds **1** and **7** bearing phenyl and 4-Cl phenyl substitution showed potent antibacterial activity

with MIC value of 10 μM and 17 μM against Gram + ve (*Staphylococcus aureus)* and MIC value of 8 μM and 13 μM against Gram –ve (*Escherichia coli)* and antifungal activity having MIC value of 10 μM and 11 μM against *Aspergillus niger* respectively. The antioxidant activity screening was carried out by *in-vitro* DPPH assay; results indicated that the compound **22** showed the most potent antioxidant activity with % scavenging activity as 77.92%. The antioxidant activity of the designed compounds is promising than the antimicrobial activity. Hence, the potential antioxidant compounds emerged from the structure activity relationship studies would be utilized for future research for the design of newer antioxidant analogs of coumarin clubbed chalcone hybrids.

Declaration of Competing Interest

The authors declare that they have no known competing financial interests or personal relationships that could have appeared to influence the work reported in this paper.

Acknowledgments

The authors thank the University grant commission, Delhi, India, Acharya Nagarjuna University College of Pharmaceutical Sciences, Acharya Nagarjuna University, Guntur, for providing the lab facilities and chemicals for this work. The authors like to acknowledge Faculty of Pharmacy, Quest International University Perak (QIUP), Malaysia, Vignan Pharmacy College, Vadlamudi, Andhra Pradesh, India, Department of Pharmaceutical Sciences, VFSTR, Vadlamudi, Andhra Pradesh, India, Dean's office of College of Pharmacy and Health Sciences, Ajman University, UAE for their support in preparation of this manuscript.

Appendix A. Supplementary material

Supplementary data to this article can be found online at https://doi.org/10.1016/j.arabjc.2021.103154.

References

Aneja, B., Arif, R., Perwez, A., Napoleon, J.V., Hasan, P., Rizvi, M. M.A., Azam, A., Rahisuddin, Abid, M., 2018. N-substituted 1,2,3-triazolyl-appended indole-chalcone hybrids as potential DNA intercalators endowed with antioxidant and anticancer properties. ChemistrySelect 3, 2638–2645. https://doi.org/https://doi.org/10.1002/slct.201702913.

Arif, R., Rana, M., Yasmeen, S., Amaduddin, Khan., Md, S., Abid, M., Khan, M.S., Rahisuddin, 2020. Facile synthesis of chalcone derivatives as antibacterial agents: Synthesis, DNA binding, molecular docking, DFT and antioxidant studies. J. Mol. Struct. 1208, 127905. https://doi.org/10.1016/j.molstruc.2020.127905.

Barot, K.P., Jain, S.V., Kremer, L., Singh, S., Ghate, M.D., 2015. Recent advances and therapeutic journey of coumarins: current status and perspectives. Med. Chem. Res. 24, 2771–2798. https://doi.org/10.1007/s00044-015-1350-8.

Bayer, A.W., Kirby, W.M.M., Sherris, J.C., Turck, M., 1966. Antibiotic susceptibility testing by a standardized single disc method. Am. J. Clin. Pathol. 45, 493–496. https://doi.org/10.1093/ajcp/45.4_ts.493.

Aksoz, B.E., Ertan, R., 2013. Chemical and structural properties of chalcones. FABAD. J. Pharm. Sci. 36, 223–242.

Beltramino, R., Penenory, A., Buceta, A.M., 2000. An open-label, randomized multicenter study comparing the efficacy and safety of Cyclo 3 Fort versus hydroxyethyl rutoside in chronic venous lymphatic insufficiency. Angiology 51, 535–544. https://doi.org/10.1177/000331970005100702.

Burch, J.D., Farand, J., Colucci, J., Sturino, C., Ducharme, Y., Friesen, R.W., Lévesque, J.F., Gagné, S., Wrona, M., Therien, A. G., Mathieu, M.C., 2011. Naphthalene/quinoline amides and sulfonylureas as potent and selective antagonists of the EP4 receptor. Bioorg. Med. Chem. Lett. 21, 1041–1046. https://doi.org/10.1016/j.bmcl.2010.12.014.

Cesar, Jesus M., García-Avello, 2004. Aging and oral anticoagulant therapy using acenocoumarol. Blood. Coagul. Fibrinolysis. 15, 673–676. DOI: 10.1097/00001721-200412000-00007

Chavan, O.S., Shioorkar, M.G., Jadhav, S.A., Sakhare, M.A., Pawar, Y.M., Chavan, S.B., Baseer, M.A., 2017. Envirocat EZP-10: an efficient catalyst for synthesis of coumarins by pechmann reaction under solvent free microwave irradiation method. Heterocycl. Lett. 7 (2), 377–380.

Dan, W., Dai, J., 2020. Recent developments of chalcones as potential antibacterial agents in medicinal chemistry. Eur. J. Med. Chem. 187,. https://doi.org/10.1016/j.ejmech.2019.111980 111980.

Patel, D., Kumari, P., Patel, N.B., 2017. Synthesis and biological evaluation of coumarin based isoxazoles, pyrimidinthiones and pyrimidin-2-ones. Arab. J. Chem. 10, S3990–S4001. https://doi.org/10.1016/j.arabjc.2014.06.010.

Djemoui, A., Naouri, A., Ouahrani, M.R., Djemoui, D., Lahcene, S., Lahrech, M.B., Boukenna, L., Albuquerque, H.M.T., Saher, L., Rocha, D.H.A., Monteiro, F.L., Helguero, L.A., Bachari, K., Talhi, O., Silva, A.M.S., 2020. A step-by-step synthesis of triazole-benzimidazole-chalcone hybrids: Anticancer activity in human cells +. J. Mol. Struct. 1204,. https://doi.org/10.1016/j.molstruc.2019.127487 127487.

Farhadi, Faegheh, Khameneh, Bahman, Iranshahi, Mehrdad, Iranshahi, Milad, 2018. Antibacterial activity of flavonoids and their structure–activity relationship: An update review. Phytother. Res. 33, 13–40. https://doi.org/10.1002/ptr.6208.

Feng, D., Zhang, A., Yang, Y., Yang, P., 2020. Coumarin-containing hybrids and their antibacterial activities. Archiv der Pharmazie 353, 1900380. 10.1002/ardp.201900380.

Fylaktakidou, K.C., Hadjipavlou-Litina, D.J., Litinas, K.E., Nicolaides, D.N., 2004. Natural and synthetic coumarin derivatives with anti-inflammatory/ antioxidant activities. Curr. Pharm. Des. 10, 3813–3833. https://doi.org/10.2174/1381612043382710.

Gao, F., Huang, G., Xiao, J., 2020. Chalcone hybrids as potential anticancer agents: Current development, mechanism of action, and structure-activity relationship. Med. Res. Rev. 40, 2049–2084. 10.1002/med.21698.

Gaudino, E.C., Tagliapietra, S., Martina, K., Palmisano, G., Cravotto, G., 2016. Recent advances and perspectives in the synthesis of bioactive coumarins. RSC. Adv. 6, 46394–46405. https://doi.org/10.1039/C6RA07071J.

Gellert, M., O'Dea, M.H., Itoh, T., Tomizawa, J., 1976. Novobiocin and coumermycin inhibit DNA supercoiling catalyzed by DNA gyrase. Proc. Natl. Acad. Sci. U S A 73, 4474–4478. https://doi.org/10.1073/pnas.73.12.4474.

Goud, N.S., Pooladanda, V., Mahammad, G.S., Jakkula, P., Gatreddi, S., Qureshi, I.A., Alvala, R., Godugu, C., Alvala, M., 2019. Synthesis and biological evaluation of morpholines linked coumarin–triazole hybrids as anticancer agents. Chem. Biol. Drug. Des. 94, 1919–1929. 10.1111/cbdd.13578.

Guan, A., Liu, C., Yang, X., Dekeyser, M., 2014. Application of the intermediate derivatization approach in agrochemical discovery. Chem. Rev. 114, 7079–7107. https://doi.org/10.1021/cr4005605.

Guoyu, Yang, Jun, Liang, 2021. The synthesis of coumarin thiazoles containing a trifluoromethyl group and their antifungal activities. Arab. J. Chem. 14. 10.1016/j.arabjc.2020.10.027..

Hajelsiddig, T.T., Saeed, A.E.M., 2015. Green chemistry approach in synthesis of 3, 4-dihydropyrimidinone derivatives under solvent-free conditions. Int. J. Pharm. Sci. Res. 6 (5), 2191. 10.13040/IJPSR.0975-8232.6(5).2191-96.

Holbrook, A.M., Pereira, J.A., Labiris, R., McDonald, H., Douketis, J.D., Crowther, M., Wells, P.S., 2005. Systematic overview of warfarin and its drug and food interactions. Arch. Intern. Med. 165, 1095–1106. https://doi.org/10.1001/archinte.165.10.1095.

Hu, X.L., Xu, Z., Liu, M.L., Feng, L.S., Zhang, G.D., 2018. Recent developments of coumarin hybrids as anti-fungal agents. CTMC 17. https://doi.org/10.2174/1568026618666171215100326.

Jakovljević, K., Joksović, M.D., Matić, I.Z., Petrović, N., Stanojković, T., Sladić, D., Vujčić, M., Janović, B., Joksović, L., Trifunović, S., Marković, V., 2018. Novel 1,3,4-thiadiazole–chalcone hybrids containing catechol moiety: synthesis, antioxidant activity, cytotoxicity and DNA interaction studies. Med. Chem. Commun. 9, 1679–1697. https://doi.org/10.1039/C8MD00316E.

Kamath, P.R., Sunil, D., Ajees, A.A., Pai, K.S.R., Das, S., 2015. Some new indole–coumarin hybrids; Synthesis, anticancer and Bcl-2 docking studies. Bioorg. Chem. 63, 101–109. https://doi.org/10.1016/j.bioorg.2015.10.001.

Kant, R., Kumar, D., Agarwal, D., Gupta, R.D., Tilak, R., Awasthi, S.K., Agarwal, A., 2016. Synthesis of newer 1,2,3-triazole linked chalcone and flavone hybrid compounds and evaluation of their antimicrobial and cytotoxic activities. Eur. J. Med. Chem. 113, 34–49. https://doi.org/10.1016/j.ejmech.2016.02.041.

Karina, Pérez-Cruz, Moncada-Basualto, Mauricio, 2018. Synthesis and antioxidant study of new polyphenolic hybrid-coumarins. Arab. J. Chem. 11, 525–537. https://doi.org/10.1016/j.arabjc.2017.05.007.

Kostopoulou, I., Diassakou, A., Kavetsou, E., Kritsi, E., Zoumpoulakis, P., Pontiki, E., Hadjipavlou-Litina, D., Detsi, A., 2020. Novel quinolinone-pyrazoline hybrids: synthesis and evaluation of antioxidant and lipoxygenase inhibitory activity. Mol. Divers. https://doi.org/10.1007/s11030-020-10045-x.

Konidala, S.K., Kotra, V., Danduga, R.C.S.R., Kola, P.K., 2020. Coumarin-chalcone hybrids targeting insulin receptor: Design, synthesis, anti-diabetic activity, and molecular docking. Bioorg. Chem. 104, 104207. https://doi.org/10.1016/j.bioorg.2020.104207

Konidala, S.K., Kotra, V., Kola, P.K., Devi, C.B.P., Anusha, N., Babu, B.H., Adil, S.F., Shaik, M.R., Khan, M., Al-Warthan, A., Alduhaish, O., 2021. ZnCl2 catalyzed new coumarinyl-chalcones as cytotoxic agents. Saudi J. Biol. Sci. 28 (1), 386–394. https://doi.org/10.1016/j.sjbs.2020.10.020.

Kraljević, T.G., Harej, A., 2016. Synthesis, in vitro anticancer and antibacterial activities and in silico studies of new 4-substituted 1,2,3-triazole-coumarin hybrids. Eur. J. Med. Chem. 124, 794–808. https://doi.org/10.1016/j.ejmech.2016.08.062.

Kurt, B.Z., Kandas, N.O., Dag, A., Sonmez, F., Kucukislamoglu, M., 2020. Synthesis and biological evaluation of novel coumarin-chalcone derivatives containing urea moiety as potential anticancer agents. Arab. J. Chem. 13 (1), 1120–1129. https://doi.org/10.1016/j.arabjc.2017.10.001.

Lagu, S.B., Yejella, R.P., Bhandare, R.R., Shaik, A.B., 2020. Design, synthesis, and antibacterial and antifungal activities of novel trifluoromethyl and trifluoromethoxy substituted chalcone derivatives. Pharmaceuticals 13 (11), 375. https://doi.org/10.3390/ph13110375.

Lagu, S.B., Yejella, R.P., Nissankararao, S., Shaik, A.B., 2019. Synthesis, antibacterial, antifungal antitubercular activities and molecular docking studies of nitrophenyl derivatives. Int. J. Life Sci. Pharma Res. 9, 54–64. 10.22376/ijpbs/lpr.2019.9.1.P54-64.

Latif, A.D., Jernei, T., Podolski-Renić, A., Kuo, C.-Y., Vágvölgyi, M., Girst, G., Zupkó, I., Develi, S., Ulukaya, E., Wang, H.-C., Pešić, M., Csámpai, A., Hunyadi, A., 2020. Protoflavone-chalcone hybrids exhibit enhanced antitumor action through modulating redox balance, depolarizing the mitochondrial membrane, and inhibiting ATR-dependent signaling. Antioxidants (Basel) 9. https://doi.org/10.3390/antiox9060519.

Lipeeva, A.V., Zakharov, D.O., 2019. Design, synthesis and antibacterial activity of coumarin-1,2,3-triazole hybrids obtained from natural furocoumarin peucedanin. Europe PMC 24. https://doi.org/10.3390/molecules24112126.

Liu, C., Guan, A., Yang, Jindong, Chai, B., Li, M., Li, H., Yang, Jichun, Xie, Y., 2016. Efficient approach to discover novel agrochemical candidates: intermediate derivatization method. J. Agric. Food Chem. 64, 45–51. https://doi.org/10.1021/jf5054707.

Lokesh, B.V.S., Prasad, Y.R., Shaik, A.B., 2017. Synthesis and biological activity of novel 2, 5-dichloro-3-acetylthiophene chalcone derivatives. Indian. J. Pharm. Educ. Res. 51 (4s), s679–s690. https://doi.org/10.5530/ijper.51.4s.99.

Akkulu Naidu, M., Rajendra Prasad, Y., 2018. Synthesis of novel diarylsulfonylurea-chalcone hybrid molecules with potential in vitro antimicrobial activity. Asian J. Pharm. 12, 88–93. 10.22377/ajp.v12i02.2320.

Potdar, M.K., Rasalkar, M.S., Mohile, S.S., Salunkhe, M.M., 2005. Convenient and efficient protocols for coumarin synthesis via Pechmann condensation in neutral ionic liquids. J. Mol. Catal. A: Chem. 235 (1–2), 249–252. https://doi.org/10.1016/j.molcata.2005.04.007.

Matos, M.J., Mura, F., Vazquez-Rodriguez, S., Borges, F., Santana, L., Uriarte, E., Olea-Azar, C., 2015. Study of coumarin-resveratrol hybrids as potent antioxidant compounds. Molecules. 20, 3290–3308. https://doi.org/10.3390/molecules20023290.

Mellado, M., Espinoza, L., Madrid, A., Mella, J., Chávez-Weisser, E., Diaz, K., Cuellar, M., 2020. Design, synthesis, antifungal activity, and structure-activity relationship studies of chalcones and hybrid dihydrochromane-chalcones. Mol. Divers. 24, 603–615. https://doi.org/10.1007/s11030-019-09967-y.

Mensor, L.L., Menezes, F.S., Leitao, G.G., Reis, A.S., dos Santos, T. C., Coube, C.S., et al, 2021. Screening of Brazilian plant extracts for antioxidant activity by the use of DPPH free radical method. Phytother. Res. 15, 127–130. https://doi.org/10.1002/ptr.687.

Menezes, J.C., Diederich, M., 2019. Translational role of natural coumarins and their derivatives as anticancer agents. Future. Med. Chem. 11, 1057–1082. https://doi.org/10.4155/fmc-2018-0375.

Mirzaei, S., Hadizadeh, F., Eisvand, F., Mosaffa, F., Ghodsi, R., 2020. Synthesis, structure-activity relationship and molecular docking studies of novel quinoline-chalcone hybrids as potential anticancer agents and tubulin inhibitors. J. Mol. Struct. 1202,. https://doi.org/10.1016/j.molstruc.2019.127310 127310.

Nagamallu, R., Srinivasan, B., Ningappa, M.B., Kariyappa, A.K., 2016. Synthesis of novel coumarin appended bis(formylpyrazole) derivatives: Studies on their antimicrobial and antioxidant activities. Bioorg. Med. Chem. Lett. 26, 690–694. https://doi.org/10.1016/j.bmcl.2015.11.038.

Osman, H., Yusufzai, S.K., Khan, M.S., Abd Razik, B.M., Sulaiman, O., Mohamad, S., Gansau, J.A., Ezzat, M.O., Parumasivam, T., Hassan, M.Z., 2018. New thiazolyl-coumarin hybrids: Design, synthesis, characterization, X-ray crystal structure, antibacterial and antiviral evaluation. J. Mol. Struct. 1166, 147–154. https://doi.org/10.1016/j.molstruc.2018.04.031.

Park, S., Kim, E.H., Kim, J., Kim, S.H., Kim, I., 2018. Biological evaluation of indolizine-chalcone hybrids as new anticancer agents. Eur. J. Med. Chem. 144, 435–443. https://doi.org/10.1016/j.ejmech.2017.12.056.

Prusty, J.S., Kumar, A., 2020. Coumarins: antifungal effectiveness and future therapeutic scope. Mol. Divers. 24, 1367–1383. https://doi.org/10.1007/s11030-019-09992-x.

Qin, H.-L., Zhang, Z.-W., Ravindar, L., Rakesh, K.P., 2020. Antibacterial activities with the structure-activity relationship of coumarin derivatives. Eur. J. Med. Chem. 207,. https://doi.org/10.1016/j.ejmech.2020.112832 112832.

Sharma, Rajesh Kumar, Katiyar, Diksha, 2019. Recent advances in the development of coumarin derivatives as antifungal agents. Recent trends in human and animal. Mycology, 235–263.

Sahu, N.K., Balbhadra, S.S., Choudhary, J., Kohli, D.V., 2012. Exploring pharmacological significance of chalcone scaffold: a review. Curr. Med. Chem. 19, 209–225. https://doi.org/10.2174/092986712803414132.

Sahoo, C.R., Sahoo, J., Mahapatra, M., Lenka, D., Sahu, P.K., Dehury, B., Padhy, R.N., Paidesetty, S.K., 2021. Coumarin derivatives as promising antibacterial agent (s). Arab. J. Chem. 14, (2). https://doi.org/10.1016/j.arabjc.2020.102922 102922.

Sanad, S.M.H., Mekky, A.E.M., 2020. Synthesis, in-vitro antibacterial and anticancer screening of novel nicotinonitrile-coumarin hybrids utilizing piperazine citrate. Synth. Commun. 50, 1468–1485. https://doi.org/10.1080/00397911.2020.1743318.

Gaonkar, Santosh L., Nagaraj, Vignesh Udyavara, 2017. Synthesis and pharmacological properties of chalcones: a review. Res. Chem. Intermed. 43, 6043. https://doi.org/10.1007/s11164-017-2977-5.

Sashidhara, K.V., Rao, K.B., Kushwaha, P., Modukuri, R.K., Singh, P., Soni, I., Shukla, P.K., Chopra, S., Pasupuleti, M., 2015. Novel chalcone-thiazole hybrids as potent inhibitors of drug resistant *Staphylococcus aureus*. ACS. Med. Chem. Lett. 6, 809–813. https://doi.org/10.1021/acsmedchemlett.5b00169.

Habib, Seema I., 2018. Chemical and biological potential of chalcones as a source of drug: A review. IJPPR. 11, 105–118.

Şenocak, A., Köksoy, B., Demirbaş, E., Basova, T., Durmuş, M., 2018. 3D SWCNTs-coumarin hybrid material for ultra-sensitive determination of quercetin antioxidant capacity. Sens. Actuators. B. Chem. 267, 165–173. https://doi.org/10.1016/j.snb.2018.04.012.

Shaik, A.B., Yejella, R.P., Shaik, S., 2017. Synthesis, antimicrobial, and computational evaluation of novel isobutylchalcones as antimicrobial agents. Int. J. Medicinal Chem. 2017. https://doi.org/10.1155/2017/6873924.

Shaik, A.B., Lohitha, K., Vani, S., Babu, P.S., 2019. Synthesis and screening of novel lipophilic diarylpropeones as prospective anti-tubercular, antibacterial and antifungal agents. Biointerface Res. Appl. Chem. 9, 3912–3918. 10.33263/BRIAC93.912918.

Shaik, A.B., Prasad, Y.R., Shahanaaz, S., 2015. Design, facile synthesis, characterization and computational evaluation of novel isobutylchalcones as cytotoxic agents: part-A. FABAD. J. Pharm. Sci. 40 (1), 1–16. https://doi.org/10.1155/2017/6873924.

Shaik, A.B., Bhandare, R.R., Nissankararao, S., Edis, Z., Tangirala, N.R., Shahanaaz, S., Rahman, M.M., 2020a. Design, facile synthesis and characterization of dichloro substituted chalcones and dihydropyrazole derivatives for their antifungal, antitubercular and antiproliferative Activities. Molecules 25, 3188. https://doi.org/10.3390/molecules25143188.

Shaik, A., Bhandare, R.R., Palleapati, K., Nissankararao, S., Kancharlapalli, V., Shaik, S., 2020b. Antimicrobial, antioxidant, and anticancer activities of some novel isoxazole ring containing chalcone and dihydropyrazole derivatives. Molecules 25, 1047. https://doi.org/10.3390/molecules25051047.

Shi, D.-H., Min, W., Song, M., Si, X.-X., Li, M.-C., Zhang, Z., Liu, Y.-W., Liu, W.-W., 2020. Synthesis, characterization, crystal structure and evaluation of four carbazole-coumarin hybrids as multifunctional agents for the treatment of Alzheimer's disease. J. Mol. Struc. 1209,. https://doi.org/10.1016/j.molstruc.2020.127897 127897.

Shigeru, M., Makoto, M., Hironaka, A., Susumu, O., 1991. Inhibition of gastric H^+, K^+-ATPase by the anti-ulcer agent, sofalcone. Biochem. Pharmacol. 42, 1447–1451. https://doi.org/10.1016/0006-2952(91)90458-H.

Singh, G., Arora, A., Kalra, P., Maurya, I.K., 2018. A strategic approach to the synthesis of ferrocene appended chalcone linked triazole allied organosilatranes: Antibacterial, antifungal, antiparasitic and antioxidant studies. Bioorg. Med. Chem. 27, 188–195. https://doi.org/10.1016/j.bmc.2018.11.038.

Sökmen, M., Khan, M.A., 2016. The antioxidant activity of some curcuminoids and chalcones. Inflammopharmacology. 24, 81–86. https://doi.org/10.1007/s10787-016-0264-5.

Song, X.F., Fan, J., Liu, L., Liu, X.F., Gao, F., 2020. Coumarin derivatives with anticancer activities: An update. Archiv. Der. Pharmazie. 353, 2000025. 10.1002/ardp.202000025.

Sribalan, R., Banuppriya, G., Kirubavathi, M., 2016. Multiple biological activities and molecular docking studies of newly synthesized 3-(pyridin-4-yl)-1H-pyrazole-5-carboxamide chalcone hybrids. Bioorg. Med. Chem. Lett. 26, 5624–5630. https://doi.org/10.1016/j.bmcl.2016.10.075.

Srikrishna, D., Godugu, C., Dubey, P.K., 2018. A review on pharmacological properties of coumarins. MRMC 18. https://doi.org/10.2174/1389557516666160801094919.

Sugino, A., Higgins, N.P., Brown, P.O., Peebles, C.L., Cozzarelli, N. R., 1978. Energy coupling in DNA gyrase and the mechanism of action of novobiocin. Proc. Natl. Acad. Sci. USA 75, 4838–4842. https://doi.org/10.1073/pnas.75.10.4838.

Ufer, M., 2005. Comparative pharmacokinetics of vitamin K antagonists: warfarin, phenprocoumon and acenocoumarol. Clin. Pharmacokinet. 44, 1227–1246. https://doi.org/10.2165/00003088-200544120-00003.

Vazquez-Rodriguez, S., Lama, L.R., Matos, M.J., 2015. Design, synthesis and antibacterial study of new potent and selective coumarin-chalcone derivatives for the treatment of tenacibaculosis. Bioorg. Med. Chem. 23, 7045–7052. https://doi.org/10.1016/j.bmc.2015.09.028.

Venugopala, K.N., Rashmi, V., Odhav, B., 2013. Review on natural coumarin lead compounds for their pharmacological activity. Biomed. Res. Int. 2013. https://doi.org/10.1155/2013/963248.

Viegas-Junior, C., Danuello, A., da Silva Bolzani, V., Barreiro, E.J., Fraga, C.A.M., 2007. Molecular hybridization: a useful tool in the design of new drug prototypes. Curr. Med. Chem. 14, 1829–1852. https://doi.org/10.2174/092986707781058805.

Vijaya, B.M., Shashikala, P., Sumakanth, M., 2017. Coumarins and chromones: A remarkable scaffolds for anti-inflammatory activity. Pharm. Sci. & Res 9, 1483–1489.

Wang, Y., Zhang, W., Dhong, J., 2019. Design, synthesis and bioactivity evaluation of coumarin-chalcone hybrids as potential anticancer agents. Bioorg. Chem. https://doi.org/10.1016/j.bioorg.2019.103530.

Wang, Y.H., Jiang, S.C., Chen, Y., Guo, T., Xia, R.J., Tang, X., He, M., Xue, W., 2019. Synthesis and antibacterial activity of novel chalcone derivatives bearing a coumarin moiety. Chem. Pap. 73, 2493–2500. https://doi.org/10.1007/s11696-019-00802-0.

Wei, H., Ruan, J., Zhang, X., 2016. Coumarin–chalcone hybrids: promising agents with diverse pharmacological properties. RSC. Adv. 6, 10846–10860. https://doi.org/10.1039/C5RA26294A.

Xu, Z., Zhao, S., Lv, Z., Gao, F., Wang, Y., Zhang, F., Bai, L., Deng, J., Wang, Q., Fan, Y., 2019. Design, synthesis, and evaluation of tetraethylene glycol-tethered isatin–1,2,3-triazole–coumarin hybrids as novel anticancer agents. J. Heterocyclic. Chem. 56, 1127–1132. https://doi.org/10.1002/jhet.3475.

Xue, Y., Liu, Yunping, Luo, Q., Wang, H., Chen, R., Liu, Yin, Li, Y., 2018. Antiradical activity and mechanism of coumarin-chalcone hybrids: theoretical insights. J. Phys. Chem. A. 122, 8520–8529. https://doi.org/10.1021/acs.jpca.8b06787.

Yazdan, S.K., Vidya Sagar, G., Shaik, A.B., 2015. Biological and synthetic potentiality of Chalcones. J. Chem. Pharm. Res. 7, 829–842.

Zhang, L., Xu, Z., 2019. Coumarin-containing hybrids and their anticancer activities. Eur. J. Med. Chem. 181,. https://doi.org/10.1016/j.ejmech.2019.111587 111587.

Zhang, S., Tan, X., Liang, C., Zhang, W., 2021. Design, synthesis, and antifungal evaluation of novel coumarin-pyrrole hybrids. J. Heterocycl. Chem. 58, 450–458. 10.1002/jhet.4180.

Zhuang, C., Zhang, Wen, Sheng, C., Zhang, Wannian, Xing, C., Miao, Z., 2017. Chalcone: A privileged structure in medicinal chemistry. Chem. Rev. 117, 7762–7810. https://doi.org/10.1021/acs.chemrev.7b00020.